Matrix Isolation Infrared and Theoretical Study of the Reaction of VCl_4 with NH_3 and $(CH_3)_3N$

David A. Kayser and Bruce S. Ault*

Department of Chemistry, University of Cincinnati, P.O. Box 210172, Cincinnati, Ohio 45221

Received: February 25, 2004; In Final Form: April 23, 2004

Initial and secondary intermediates in the reaction of VCl_4 with NH_3 have been characterized by matrix isolation infrared spectroscopy and density functional calculations. Twin jet codeposition of these two reagents led to a series of moderately intense infrared absorptions that have been assigned to the 1:1 molecular complex between these two species. Irradiation of these matrices with light of $\lambda > 300$ nm led to complete destruction of the complex, and the growth of a number of new bands. These have been assigned to the Cl_3VNH_2 species, complexed with a single HCl arising from destruction of the complex. Identification of these species (1:1 complex and photoproduct) was supported by extensive isotopic labeling (^{15}N and ^2H), as well as by B3LYP/6−311++g(d, 2p) density functional calculations. Good agreement was observed between the experimental and computed frequencies. The binding energy of the 1:1 complex was calculated to be $\Delta E^{\circ}_{298} = -11.43$ kcal/mol at this level of theory. Similar experiments with $(CH_3)_3N$ led to no detectable products.

Introduction

High valent transition metal oxo compounds, including $OVCl_3$, $CrCl_2O_2$, and $MoOCl_4$, are very strong oxidizing agents and are known to oxidize a wide range of organic substrates.[1,2] This oxidizing power has applications in catalysis as well as in organic synthesis. Despite the utility of these reagents, the mechanism of oxidation is not well understood, although progress has been made in recent years. Of particular interest is the reaction chemistry of VCl_4, which might be expected to be similar to that of its oxo counterpart, $OVCl_3$. However, two significant differences are present. First is the presence of the oxo group, and the second is the presence of an unpaired electron on the vanadium center in VCl_4, with an expected Jahn−Teller distortion. This distortion has been confirmed, both by matrix esr studies[3] and theoretical calculations.[4]

The matrix isolation technique[5−7] was developed to facilitate the isolation and spectroscopic characterization of reactive intermediates. This approach has been applied to the study of a wide range of species, including radicals, weakly bound molecular complexes, and molecular ions. A recent series of matrix isolation studies[8−12] has examined the reactions of both $OVCl_3$ and $CrCl_2O_2$ with small molecules, including H_2O, CH_3OH, CH_3SH and NH_3. For each system, a sequence of intermediate species was observed, from the initially formed 1:1 molecular complex to the thermally- or photochemically-induced HCl elimination product. Very recently, a matrix isolation study[4] in this laboratory explored the reaction of VCl_4 with CH_3OH, leading to the identification of Cl_3VOCH_3 and an initial comparison of the reactivities of VCl_4 and $OVCl_3$. To extend this investigation, a matrix isolation infrared spectroscopic study was undertaken, to explore the range of reaction products of VCl_4 with ammonia and with trimethylamine in argon matrices. Theoretical calculations were carried out in support of the experimental work.

Experimental Details

All of the experiments in this study were conducted on the conventional matrix isolation apparatus that has been described.[13] Vanadium (IV) chloride, VCl_4, (Aldrich) was introduced into the vacuum system by placing a few drops of the neat liquid in a small stainless steel sidearm, connected to the deposition line through a needle valve to an UltraTorr tee. The needle valve was opened slightly, allowing a fraction of the vapor pressure of VCl_4 at room temperature to be entrained in flowing argon, carried to the cold window, and deposited. With this method of deposition, the precise concentration of VCl_4 in solid argon could not be determined. With a room-temperature vapor pressure of several mmHg, the amount of VCl_4 deposited is determined by the flow of this vapor pressure through the needle valve. Based on band intensity comparisons to $OVCl_3$, the concentrations were estimated to be in the range 250/1 to 1000/1. NH_3 (Matheson), $^{15}NH_3$, ND_3 (both from Cambridge Isotope Laboratories, 99% isotopic enrichment) and $(CH_3)_3N$ (Aldrich) were introduced into the vacuum system from lecture bottles, and purified by repeated freeze−pump−thaw cycles. Argon was used as the matrix gas in all experiments, and was used without further purification.

Matrix samples were deposited in both the twin jet and merged jet modes. In the former, the two gas samples were deposited from separate nozzles onto the 14 K cold window, allowing for only a very brief mixing time prior to matrix deposition. Several of these matrices were subsequently warmed to 33−35 K to permit limited diffusion and then recooled to 14 K and additional spectra recorded. In addition, most of these matrices were irradiated with the H_2O/Pyrex-filtered output of a 200 W medium-pressure Hg arc lamp, after which additional spectra were recorded. Irradiation times between 1 and 3 h were used.

Many experiments were conducted in the merged jet mode,[14] in which the two deposition lines were joined with an UltraTorr tee at a distance from the cryogenic surface, and the flowing gas samples were permitted to mix and react during passage through the merged region. The length of this region was variable between 10 and 90 cm. In both twin and merged jet, matrices were deposited at the rate of 2 mmol/hr from each sample manifold onto the cold window. Final spectra were

10.1021/jp0491459 CCC: $27.50

TABLE 1: Band Positions* and Assignments for the 1:1 Complex of VCl_4 with NH_3 and Its Isotopomers

$VCl_4-{}^{14}NH_3$	$VCl_4-{}^{15}NH_3$	$VCl_4-{}^{14}NH_2D$	$VCl_4-{}^{14}NHD_2$	$VCl_4-{}^{14}ND_3$	parent	assignment
424 cm^{-1}	424	424	424	424	474	V−Cl st.
440	440	436	436	436	501	V−Cl st.
696	693					NH_3 rock
1197	1191	1116	983	924	974	NH_3 sym. bend
1598	1595				1621	NH_3 antisym. bend
3296	3293		2539	2532	3330	NH_3 sym. stretch
3395	3386		3395		3440	NH_3 antisym. stretch

*Set A bands, see text.

TABLE 2: Band Positions* and Assignments for Argon Matrix Isolation Cl_3VNH_2

Cl_3VNH_2	$Cl_3V^{15}NH_2$	Cl_3VNHD	Cl_3VND_2	assignment
453 cm^{-1}	451			VCl_2 antisym. stretch
581	572			NH_2 twist
729	714	718	682	V−N stretch
1419	1410			NH_2 bend
3317	3313	2458	2420	NH_2 sym. stretch
			2543	NH_2 antisym. stretch

*Set B bands, see text.

recorded on a Perkin-Elmer Spectrum One Fourier transform infrared spectrometer at 1 cm^{-1} resolution.

Theoretical calculations were carried out on a number of possible intermediates in this study, using the Gaussian 03W suite of programs.[15] Several different model chemistries were employed, including Hartree−Fock and density functional calculations. These calculations were used to locate energy minima, determine structures, and calculate vibrational spectra. Final calculations with full geometry optimization employed unrestricted B3LYP with the 6−311++g(d, 2p) basis set, after initial calculations with smaller basis sets were run to approximately locate energy minima.

Experimental Results

Prior to any codeposition experiments, blank experiments were run on each of the reagents used in this study. In each case, the blanks were in good agreement with literature spectra and with blanks run previously in this laboratory.[16−20] All experiments involving VCl_4 showed small amounts of $OVCl_3$ impurity[21] that could not be eliminated. However, since the reaction of $OVCl_3$ with NH_3 has been studied, minor bands due to this side reaction could be identified. Each blank experiment was then irradiated by the H_2O/Pyrex filtered output of a 200 W Hg arc lamp for 1.5 h. No changes were observed in any of the blank spectra as a result of irradiation. Also, weak bands due to HCl impurity were noted in all of the VCl_4 blank experiments.[22]

$VCl_4 + NH_3$. In an initial twin-jet experiment, a sample of Ar/VCl_4 was codeposited with a sample of Ar/NH_3 = 500. After 20 h of deposition, a series of new bands were observed in the spectrum, at 424, 440, 696, 1197, 1598, 3296, and 3395 cm^{-1}. These will hereafter be referred to as set A and are collected in Table 1. Several were moderately intense, particularly the 1197 cm^{-1} band, and most were quite sharp. When this matrix was subsequently annealed to about 31 K, recooled, and an additional spectrum recorded, all of these bands grew somewhat in intensity (10−15% growth). This matrix was then irradiated by the H2O/Pyrex-filtered output of a medium-pressure Hg arc (i.e. $\lambda > 300$ nm). All of the set A bands were greatly reduced in intensity, and a series of new absorptions were noted. These bands, collectively set B, were located at 453, 581 (multiplet), 729, 1419, 2757, 2767, and 3317 cm^{-1} and are collected in Table 2. In addition, quite weak bands due to the known photoproducts of the $OVCl_3$/NH_3 system were seen in the spectrum.[11]

This experiment was repeated 10−12 times, employing different concentrations of the two reagents. Overall, similar results were obtained in each experiment. The set A bands were seen upon initial deposition, with an intensity that was roughly proportional to the concentration levels of the two reagents. More importantly, the relative intensities of the bands comprising set A maintained a constant intensity ratio with respect to one another throughout these experiments. Subsequent irradiation of these matrices led to a sharp decrease in the intensity of the set A bands, along with a growth in the set B bands. In those experiments in which the set A bands were more intense, the final intensity of the set B bands after irradiation was greater than in experiments with a lower yield of the set A bands. Further, all of the bands in set B maintained a constant intensity ratio with respect to one another in these experiments. In contrast, the bands due to the photoproducts in the $OVCl_3$/NH_3 system varied in intensity relative to the set B bands, since the amount of $OVCl_3$ impurity varied from one experiment to the next.

The reaction of VCl_4 with NH_3 was also explored in two merged=jet experiments, using a room-temperature merged region (reaction zone). In these two experiments, the bands due to the parent VCl_4 and NH_3 were seen with greatly reduced intensity in the resulting spectrum (compared to the twin-jet experiments). No new bands were observed, and neither the set A or set B bands were seen. To verify that each sample was prepared correctly, the flow of the Ar/VCl_4 sample was stopped and the bands due to the parent NH_3 grew in strongly. When the Ar/NH_3 flow was stopped and the Ar/VCl_4 flow started, bands due to VCl_4 grew in strongly. In view of these results, merged-jet experiments were not conducted with the isotopically labeled NH_3 samples described below.

$VCl_4 + {}^{15}NH_3$. Samples of Ar/VCl_4 were codeposited with samples of Ar/$^{15}NH_3$ in 5−6 experiments, employing a range of sample concentrations. Due to exchange in the vacuum system with residual $^{14}NH_3$, the samples contained a mixture of ^{14}N and ^{15}N, initially in about a 1/1 ratio. In subsequent experiments, the $^{15}N/^{14}N$ ratio increased to 2/1. Consequently the product bands described above for the ^{14}N isotope were seen in all of these experiments. In addition, new product bands were seen upon initial deposition, quite near and on the low energy side of the ^{14}N set A bands. For example, a new band was seen at 1191 cm^{-1}, shifted down in energy from the 1197 cm^{-1} band observed for the normal isotope, as shown in Figure 1. Table 1 lists all of the bands in the ^{15}N counterparts of set A. Each of these matrices was then irradiated with light of $\lambda > 300$ nm. As a result of irradiation, the intensity of the initial product bands decreased significantly, and a new set of bands, analogous to the set B bands (above) grew in, as shown for one spectral region in Figure 2. Each band was shifted slightly to lower

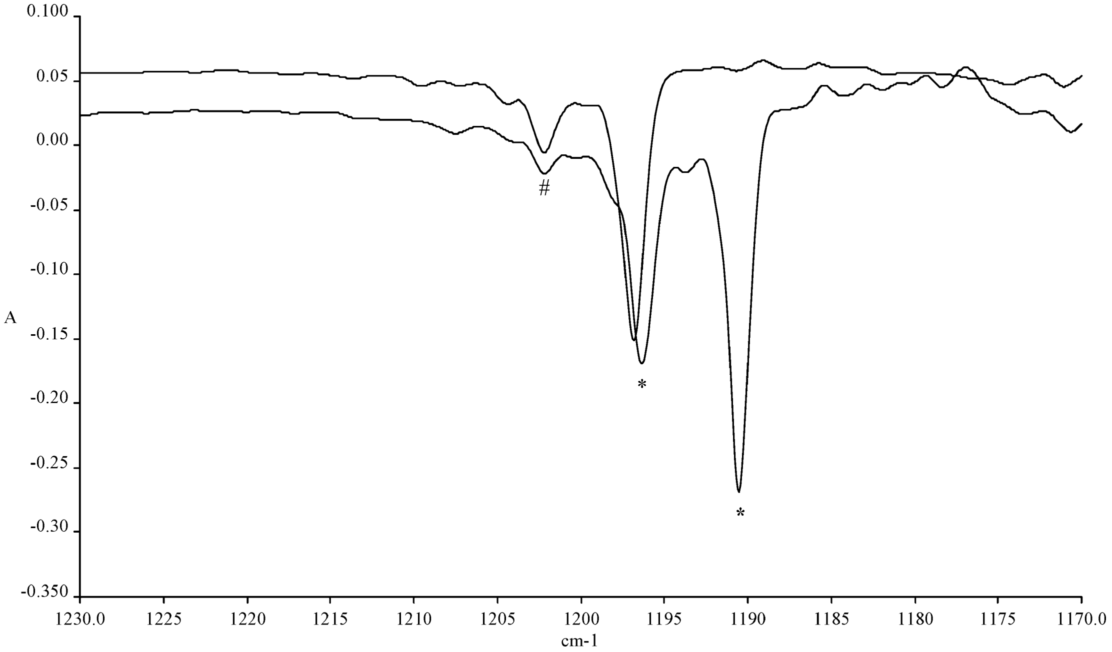

Figure 1. Difference spectra showing the decrease of the symmetric bending mode of NH_3 in the 1:1 complex Cl_4V-NH_3: upper trace uses $^{14}NH_3$, while the lower trace employes $^{15}NH_3$ (with some $^{14}NH_3$ impurity). Bands marked with an $*$ are due to Cl_4V-NH_3 while bands marked with a # are due to Cl_3VO-NH_3 from Cl_3VO impurity.

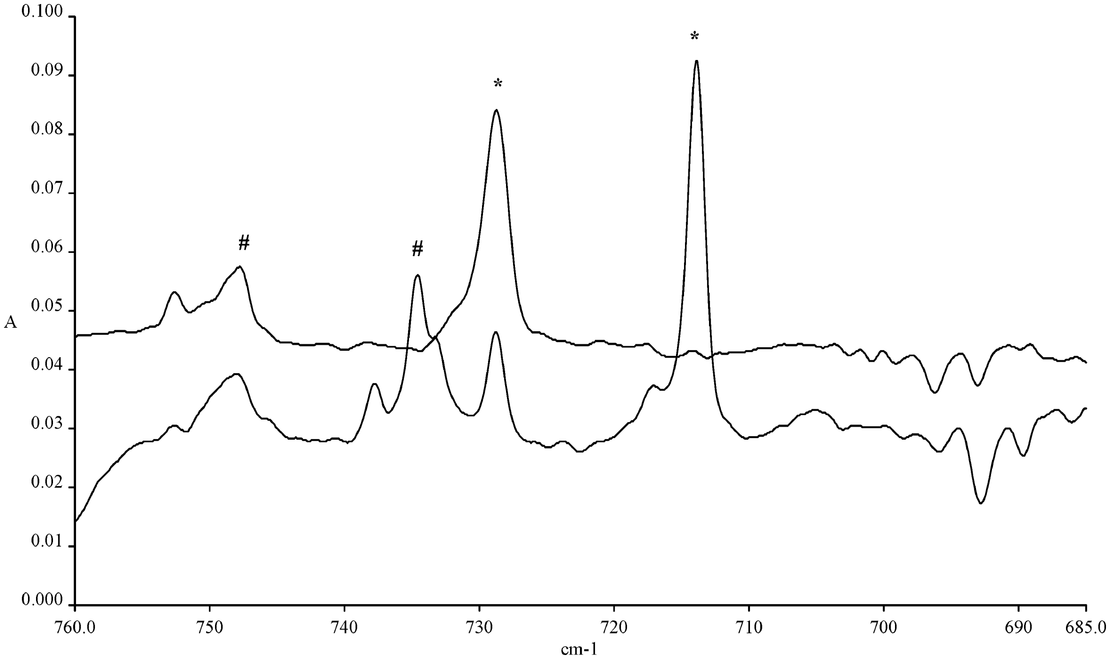

Figure 2. Difference spectra in the V−N stretching region for $Cl_3V^{14}NH_2$ (upper trace) and $Cl_3V^{15}NH_2$ (lower trace, with ^{14}N impurity). Bands marked with an $*$ are due to Cl_3VNH_2 while bands marked with a # are due to $Cl_2V(O)NH_2$ from Cl_3VO impurity.

energy from the analogous ^{14}N band, except for the doublet at 2757, 2767 cm^{-1}. This doublet did not shift with ^{15}N substitution. Table 2 lists the set B bands obtained when $^{15}NH_3$ was employed.

$VCl_4 + ND_3$. Samples of Ar/VCl_4 were codeposited with samples of Ar/ND_3 in several experiments, using twin-jet deposition. These experiments were complicated by the issue of hydrogen−deuterium isotope exchange with residual NH_3, as well as trace H_2O in the system. Consequently, samples of Ar/ND_3 contained a mixture of ND_3, ND_2H, NDH_2, and a small amount of NH_3. Further, the N−D oscillator absorbs approximately 50% as strongly as an N−H oscillator, so that overall band intensities were reduced. Consequently, fewer product bands were detected in these experiments. Nonetheless, deuterated and partially deuterated counterparts of the most intense band in set A (1197 cm^{-1}) were seen at 924, 1033, and 1116 cm^{-1}. Product bands were seen prior to irradiation at 424 and 436 cm^{-1}, as well as weak bands in the N−D and N−H stretching regions. These are all listed in Table 1 All of these bands were destroyed by Hg arc irradiation ($\lambda > 300$ nm), and several weak new product bands were detected. A number of these are listed in Table 2. In addition, a distinct doublet was observed at 1996 and 2006 cm^{-1}, with band profiles and intensities that were very similar to the 2757, 2767 cm^{-1} doublet observed with the normal isotopic material and in the ^{15}N experiments. While these experiments were particularly difficult due to low band intensities, the results were reproducible over the several experiments that were run.

TABLE 3: Calculated[a] and Experimental Band[b] Positions and Isotopic Shifts for the 1:1 Complex Cl_4V-NH_3

$VCl_4-{}^{14}NH_3$ band position			$VCl_4-{}^{15}NH_3$ shift		$VCl_4-{}^{14}NH_2D$ shift		$VCl_4-{}^{14}NHD_2$ shift		$VCl_4-{}^{14}ND_3$ shift		
calc.	expt.	I (calc)[c]	calc.	expt.	calc.	expt.	calc.	expt.	calc.	expt.	assignment
411		184									
419	424	166	−1	0		0		0	−2	0	V−Cl st.
449	440	136	0	0		−4		−4	−6	−4	V−Cl st.
667*	696	25	−	−							NH_3 rock
1248	1197	143	−	−	-88	−	−	−	−	−	NH_3 sym. bend
1660*	1598	20	−	−							NH_3 antisym. bend
3468	3296	12	−	−					−	−	NH_3 sym. stretch
3584*	3395	28	−	−							NH_3 antisym. stretch

*Doubly degenerate. [a] Calculated at the UB3LYP/6−311++g(d, 2p) level, frequencies are unscaled. [b] Band positions in cm^{-1}. [c] Intensities in km/mol.

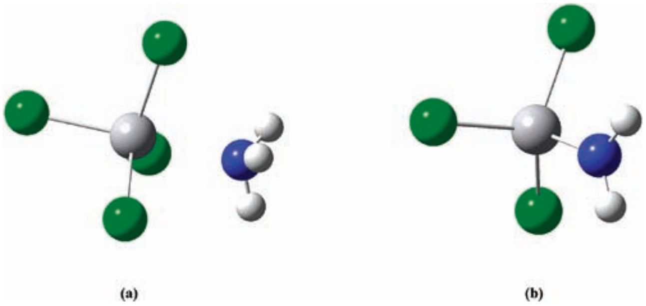

Figure 3. Calculated structures for the 1:1 complex of VCl_4 with NH_3 (a) and Cl_3VNH_2 (b).

$VCl_4 + (CH_3)_3N$. Samples of Ar/VCl_4 were codeposited with samples of Ar/$(CH_3)_3N$ = 200 in two experiments, again using twin-jet deposition. No distinct product bands were observed upon initial matrix deposition in either experiment. These matrices were then irradiated as usual. No product bands were formed as a result of irradiation, and no significant decreases were noted in any of the parent bands in the spectrum.

Results of Calculations

DFT calculations focused on energy minima, structures, and vibrational frequencies for possible reaction products. Of particular interest was the 1:1 complex between VCl_4 and NH_3, since several similar transition metal chlorides have been shown to form such complexes. This complex optimized to a stable energy minimum at all levels of theory employed, including unrestricted B3LYP/6−311++g(d,2p), the highest level employed. The structure of the complex is depicted in Figure 3. The binding energy of the complex, relative to the separated subunits, was calculated to be < $\Delta E^{\circ}_{298} = -11.43$ kcal/mol at this level of theory. Vibrational frequencies and band intensities were also calculated, for the normal isotopic species as well as the ^{15}N and deuterium isotopomers. These are listed in Table 3.

Based on previous studies,[8−12] the HCl elimination product from the complex, Cl_3VNH_2, was of interest as well. Cl_3VNH_2 optimized to a stable energy minimum at all levels of theory employed, including unrestricted UB3LYP/6−311++g(d, 2p), the highest level employed. The resulting structure was reasonable; the key geometric parameters are listed in Table 4 and the structure is shown in Figure 3. Vibrational frequencies were also calculated, for the normal isotopic species as well as for the ^{15}N, −NHD, and $-ND_2$ isotopomers. These frequencies, band intensities, and isotopic shifts are listed in Table 5. Calculations were also carried out for potential secondary products, including Cl_2VNH, that might be formed in this reaction.

TABLE 4: Calculated* Key Structural Parameters for Cl_3VNH_2 and $Cl_2V(O)NH_2$[b]

parameter	Cl_3VNH_2	$Cl_2V(O)NH_2$
R_{V-Cl}[a]	2.17 Å	2.18 Å
R_{V-N}	1.81	1.781
R_{N-H}[a]	1.01	1.01
α(Cl−V−Cl)[a]	112.5°	110.7°
α(Cl−V−N)[a]	107.1	
α(H−N−H)[a]	112.1	112.7

*Calculated at the UB3LYP/6−311++g(d, 2p) level of theory. [a] Average value. [b] From ref 11.

Discussion

Numerous product bands and several product species were isolated in the reaction of VCl_4 with NH_3 under a range of reaction conditions. As noted above, many of the product bands can be grouped into sets, based on the conditions under which they appeared, and the fact that bands within a given set maintained a constant intensity ratio with respect to other bands in that set. It is also apparent that the different product species are formed in sequence, as reaction conditions are altered and additional energy is deposited into the system. The identity of the species responsible for each set of product bands will be discussed, supported by the results of theoretical calculations and followed by an overview of the mechanism of reaction.

Product Identification

The bands in set A were formed under the conditions of shortest reaction time and lowest reaction temperature, namely in the twin-jet deposition experiments where mixing of the two reactants occurs on the surface of the condensing matrix. This indicates the species A is the initial intermediate in the reaction between VCl_4 and NH_3. It is also noteworthy that each of these bands (except for the band near 696 cm^{-1}) was observed relatively near a parent mode of either VCl_4 or NH_3. For example, the 424 and 440 cm^{-1} bands are shifted from the parent VCl_4 stretching modes at 474 and 501 cm^{-1}, while the 3296 and 3395 cm^{-1} bands lie near the NH_3 stretching modes of ammonia. Further, the isotopic dependence of each of the set A bands mirrored closely the isotopic dependence of the nearby parent mode. These observations are indicative[23] of the formation of a molecular complex between the two reacting species, where each subunit is perturbed in the complex, yet maintains its molecular identity. On this basis, the bands in set A are assigned to a molecular complex between VCl_4 and NH_3 and its isotopomers in argon matrices.

The stoichiometry of the complex is not as readily determined. However, the observation of only a single product after codeposition over a wide range of concentrations suggests that the stoichiometry is 1:1. Certainly, it would be difficult to envision formation of higher complexes (e.g., 2:1 or 1:2) without

TABLE 5: Calculated[a] and Experimental Band[b] Positions and Isotopic Shifts for Cl_3VNH_2

Cl_3VNH_2 band position			$Cl_3V^{15}NH_2$ shift		Cl_3VNHD shift		Cl_3VND_2 shift		
calc.	expt.	I[c] (calc.)	calc.	expt.	calc.	expt.	calc.	expt.	assignment
459	453	111	0	−2					V−Cl stretch
468		43							V−Cl stretch
541	581	255	−4	−9					NH_2 twist
626		53							NH_2 twist
748	729	76	−15	−15	−11	−11	−48	−47	V−N stretch
1532	1419	45	−5	−9					NH_2 bend
3504	3317	100	−5	−4			−975	−897	NH_2 sym. stretch
3609		36							NH_2 antisym. stretch

[a] Calculated at the UB3LYP/6−311++g(d, 2p) level, frequencies are unscaled. [b] Band positions in cm^{-1}. [c] Intensities in km/mol.

also forming the 1:1 complex. The observation of a single product argues against this, and for the formation of the 1:1 complex. This conclusion is strongly supported by the density functional calculations that concluded that the 1:1 complex is bound by approximately 11.4 kcal/mol at the UB3LYP/6−311++g(d, 2p) level of theory. More importantly, the frequencies calculated for the 1:1 complex are in quite good agreement with the experimental values and the isotopic shifts. An example is the symmetric deformation or "umbrella" mode of NH_3, ν_2. This mode, ν_2, has been shown many times[24,25] to be extremely sensitive to complexation, and to shift to higher energy upon complex formation. In hydrogen bonding interactions, this mode has been observed to shift 25−100 cm^{-1} to higher energy, while in a Lewis acid−base complex, shifts of up to 400 cm^{-1} to higher energy have been observed; shifts of 200 cm^{-1} are typical. This mode is calculated to shift $1248 - 1026 = +222$ cm^{-1} to higher energy from the parent band position, while a shift of $1197 - 974 = +223$ cm^{-1} was observed. The calculated isotopic shifts of this mode are shown in Table 3, and are quite close to the experimental shifts, when anharmonicity is taken into account. Also, this mode is calculated to be the most intense absorption of the 1:1 complex, and the 1197 cm^{-1} was in fact the most intense band in set A. The other bands observed for the complex are in good agreement with the calculated spectra for the 1:1 complex. Consequently, the set A bands described above are assigned to the 1:1 molecular complex between VCl_4 and NH_3. *This species represents the initial intermediate in the reaction between these two compounds*.

The 1:1 molecular complex is clearly very sensitive to ultraviolet irradiation, as bands due to this complex were completely destroyed by irradiation with light of $\lambda > 300$ nm. Similar results were observed for the $OVCl_3{\cdot}NH_3$, and $CrCl_2O_2{\cdot}O(H)CH_3$ complexes, as well as several related complexes. In each of these cases, it was shown conclusively that complex destruction occurred through HCl elimination, after absorption of a photon. The HCl produced in these systems, however, was trapped within the matrix cage with the second photoproduct ($Cl_2V(O)NH_2$ and $ClCr(O)_2OCH_3$, respectively). The HCl spectrum, then, was that of weakly hydrogen bonded HCl, with bands appearing near 2750 cm^{-1}. Similar absorptions were seen in the present experiments, at 2757 and 2767 cm^{-1}. These bands did not shift upon ^{15}N substitution, but did shift to 1996 and 2006 cm^{-1} upon deuteration. This is precisely the isotopic dependence anticipated for HCl. In addition, the ν_H/ν_D ratio of $2767/2006 = 1.38$ is identical to that observed for both gas phase and matrix isolated[26] HCl, namely 1.38. Thus, this doublet is assigned to photoproduced HCl, arising from the decomposition of the initial 1:1 molecular complex. Further, the HCl that is produced is trapped within the same matrix cage, and weakly hydrogen bonded to the species responsible for the set B bands.

Species B is clearly identified with the species resulting from an HCl elimination process from the molecular complex. In several of the previously studied systems (e.g. $CrCl_2O_2 + CH_3OH$), only one HCl elimination product was possible. This was the product arising from the elimination of one HCl unit from the complex, yielding (in that case) $ClCr(O)_2OCH_3$. However, in the present case the possibility of the elimination of one, two, or even three HCl units from the molecular complex is present (as it was in the $OVCl_3/NH_3$ system), to yield Cl_3VNH_2, Cl_2VNH, and ClVN, respectively. The bands due to species B maintained a constant intensity ratio in all of the experiments (as best this could be determined with the low band intensities that were observed), including different irradiation times and different sample concentrations. This indicates that probably only one product (other than HCl) is observed upon irradiation. This was the result obtained for the $OVCl_3/NH_3$ system.

ClVN can be ruled out on the basis that several of the set B product bands shifted upon deuteration, yet ClVN has no hydrogen atoms. Thus, ClVN cannot be responsible for the set B bands. The second species, Cl_2VNH, would have one N−H stretching band (and it's deuterium counterpart would have one N−D stretching band). However, in the VCl4 + ND_3 experiments three bands were observed in the N−D stretching region, arguing against assignment to this species. However, the first species Cl_3VNH_2 is consistent with all of these observations. In the N−D stretching region, two N−D stretches are anticipated for Cl_3VND_2. In addition, the mixed species [Cl_3VNHD] should be formed at the level of isotopic enrichment employed here, which would contribute a third band in the N−D stretching region.

To further distinguish between these two possibilities (Cl_3VNH_2 versus Cl_2VNH), theoretical calculations were undertaken. The calculated spectra of these two species were compared to the experimental spectrum; as shown below, the fit to the computed spectrum of Cl_3VNH_2 is much better. Further, the observed band intensities of set B match well the calculated intensities should in Table 5. The four bands of Cl_3VNH_2 calculated to have the highest intensity were observed, along with one weaker band. Therefore, the bands in set B, as listed in Table 2, are assigned to the single HCl elimination product from the 1:1 molecular complex, namely Cl_3VNH_2. *This marks the first observation of this intermediate in the VCl_4/NH_3 reaction system.*

Band Assignments

Band assignments for 7 of the 8 observed bands of the 1:1 complex are straightforward, based on their proximity to parent modes. These assignments are collected in Table 1, for the complexes of VCl_4 with NH_3, $^{15}NH_3$, and ND_3. In addition, one new band (the 8th band) was formed as a result of complexation, at 696 cm^{-1}. This band does not have its origins in a parent mode of either of the subunits in the complex. Rather, studies have shown[24] that complexed NH_3 undergoes a rocking motion when complexed; this motion has been observed[27] near 700 cm^{-1} for moderately-strongly bound complexes of NH_3. This (and 5 lower frequency modes) arise from the loss of 3 translational and 3 rotational degrees of freedom upon complex formation. The others, including the V−N stretching mode, are expected to lie below the 400 cm^{-1} cutoff of the infrared spectrometer. This mode was calculated to come at 667 cm^{-1}, with a 3 cm^{-1} red shift with ^{15}N substitution. While the experimental frequency is slightly higher than the calculated value, the calculated isotopic shift is identical to the experimental value.

Theoretical calculations for both Cl_2VNH and Cl_3VNH_2 can be compared to experimental results. Of course, with fewer atoms, Cl_2VNH is calculated to have 4 fundamentals above 400 cm^{-1}, the instrumental cutoff. These are calculated at 494, 582, 1029, and 3559 cm^{-1}, all with substantial infrared intensity. Clearly, this species cannot account for all of the observed product bands (for example, the bands at 729 and 1419 cm^{-1}). Three of the calculated bands fall very near intense bands of the parent species, and conceivably could escape detection. The last, at 582 cm^{-1}, is near a weak product band, although it should be noted that Cl_3VNH_2 is also calculated to have a product band in this region. Thus, while the possible formation of Cl_2VNH cannot be ruled out, this species cannot account for a number of the observed bands and another species must be formed as a result of irradiation.

The calculated spectrum of Cl_3VNH_2 is in good overall agreement with the observed spectrum, including isotopic shifts, as shown in Table 5. Of particular note is the V−N stretching mode, calculated at 748 cm^{-1} and observed at 729 cm^{-1}. The calculated isotopic shifts of this mode for $Cl_3V^{15}NH_2$, Cl_3VNHD, and Cl_3VND_2 were −15, −11, and −48 cm^{-1}, respectively, while the experimental shifts were −15, −11, and −47 cm^{-1}, a nearly perfect fit. The remaining isotopic shift comparisons are quite reasonable, where observed, although not as good as these. Overall, assignment to Cl_3VNH_2 is made, with the band assignments listed in Table 2.

Further Considerations

Several matrix isolation studies[8−12] of the reaction mechanism of $OVCl_3$ and $CrCl_2O_2$ with small molecules have all suggested that the first step in the reaction is the formation of a molecular complex, for those small molecules containing a heteroatom (N, O, P, S). This agrees with theoretical calculations as well. The second step in each system studied has been HCl elimination, whenever 1 or more active hydrogen was present. In several cases, this was observed to occur thermally, in a merged-jet system, while in other cases (including the present study), the reaction was photochemically induced. For those systems that were photochemically driven to eliminate HCl, two different circumstances were noted in the merged-jet experiment. In the first, typified by the $OVCl_3/CH_3SH$ system, no reaction was observed during the merged-jet experiments. This suggests that the initial molecular complex is sufficiently weakly bound that the complex is largely dissociated in the gas phase at room temperature, so that subsequent HCl elimination cannot occur. Here, the cryogenic temperature of the matrix is required to produce significant amounts of the complex, and then photochemical excitation is needed.

In the second circumstance, including the present VCl_4/NH_3 study, complete reaction appears to occur in the merged-jet region, with no intermediates or products reaching the cold window. In the present study, it was clear that both reagents were present in the merged region, since when the VCl_4 stream was turned off, bands due to NH_3 grew in the matrix spectrum thereafter. It is likely that the complex forms in the gas phase, and while it is relatively strongly bound, the barrier to HCl elimination and then to further reaction is low. Thus, the first and second intermediates are formed and destroyed in the merged region, and only nonvolatile stable products are produced. In these cases, it is difficult to prove that the same sequence of intermediates (i.e., mechanism) occurs in the thermal reaction and the photochemical reaction. However, in at least one case,[11,28] it has been shown clearly that the thermal and photochemical reactions follow the same pathway. While not proven, it is likely here as well.

It is noteworthy that the twin-jet codeposition of $Ar/(CH_3)_3N$ with Ar/VCl_4 led to essentially no product bands. Certainly, $(CH_3)_3N$ is known[29] to be more basic than NH_3, so that complexation is anticipated. However, $(CH_3)_3N$ is much bulkier than NH_3, and the region around the vanadium center may be too sterically congested to permit formation of detectable amounts of the molecular complex.

A comparison of the experimental spectrum of Cl_3VNH_2 observed here with that of $Cl_2V(O)NH_2$ observed previously through the photochemical reaction of NH_3 with $OVCl_3$ is of interest. Where comparable modes are present in both species, they are located very close to one another. For example, the V−N stretching modes are located at 748 and 729 cm-1 for $Cl_2V(O)NH_2$ and Cl_3VNH_2, respectively, while the NH_2 symmetric stretching modes were located at 1330 and 1317 cm^{-1}, respectively. The overall yield was lower in the present study, probably a consequence of the greater difficulty in handling VCl_4 as compared to $OVCl_3$. Similar observations may be made concerning the 1:1 complexes of NH_3 with VCl_4 and $OVCl_3$; for example, ν_2 of NH_3 was observed at 1202 cm^{-1} in the $OVCl_3$ complex and at 1197 cm^{-1} in the VCl_4 complex. Overall, the reactivities and intermediates are quite similar, suggesting that the oxo group on $OVCl_3$ does not play a major role in these reactions. Likewise, the lone electron on the vanadium center in VCl_4, and subsequent Jahn−Teller distortion, do not significantly affect the intermediates that are formed. These conclusions are in agreement with the recent study[4] of the reaction of VCl_4 with CH_3OH.

Acknowledgment. The National Science Foundation is gratefully acknowledged for their support of this research through grant CHE02-43731.

References and Notes

(1) Crans, D. C.; Chen, H.; Felty, R. A. *J. Am. Chem. Soc.* **1992**, *114*, 4543.
(2) Yajima, A.; Matsuzaki, R.; Saeki, Y. *Bull Chem. Soc. Jpn*. **1978**, *51*, 1098.
(3) Graham, J. T.; Li, L.; Weltner, W., Jr. *J. Phys. Chem. A.* **2000**, *104*, 9302.
(4) Sabestinas, D; Ault, B. S. *J. Phys. Chem*., submitted.
(5) Craddock, S.; Hinchliffe, A., *Matrix Isolation*; Cambridge University Press: Cambridge, 1975.
(6) Hallam, H. E.; *Vibrational Spectroscopy of Trapped Species*; John Wiley: New York, 1973.
(7) *Chemistry and Physics of Matrix Isolated Species*; Andrews, L., Moskovitz, M., Eds.; Elsevier Science Publishers: Amsterdam, 1989.
(8) Ault, B. S. *J. Am. Chem. Soc*. **1998**, *120*, 6105.
(9) Anderson, S. R.; Ault, B. S. *J. Phys. Chem. A* **2002**, *106*, 1419.
(10) Ault, B. S. *J. Phys. Chem. A* **1999**, *103*, 11474.
(11) Ault, B. S. *J. Phys. Chem. A* **2001**, *105*, 4758.
(12) Subel, B. L.; Kayser, D. A.; Ault, B. S. *J. Phys. Chem. A.* **2002**, *106*, 4998.
(13) Ault, B. S. *J. Am. Chem. Soc.* **1978**, *100*, 2426.
(14) Carpenter, J. D.; Ault, B. S. *J. Phys. Chem.* **1991**, *95*, 3502.
(15) Frisch, M. J.; Trucks, G. W.; Schlegel, H. B.; Scuseria, G. E.; Robb, M. A.; Cheeseman, J. R.; Montgomery, J. A., Jr.; Vreven, T.; Kudin, K. N.; Burant, J. C.; Millam, J. M.; Iyengar, S. S.; Tomasi, J.; Barone, V.;

Mennucci, B.; Cossi, M.; Scalmani, G.; Rega, N.; Petersson, G. A.; Nakatsuji, H.; Hada, M.; Ehara, M.; Toyota, K.; Fukuda, R.; Hasegawa, J.; Ishida, M.; Nakajima, T.; Honda, Y.; Kitao, O.; Nakai, H.; Klene, M.; Li, X.; Knox, J. E.; Hratchian, H. P.; Cross, J. B.; Adamo, C.; Jaramillo, J.; Gomperts, R.; Stratmann, R. E.; Yazyev, O.; Austin, A. J.; Cammi, R.; Pomelli, C.; Ochterski, J. W.; Ayala, P. Y.; Morokuma, K.; Voth, G. A.; Salvador, P.; Dannenberg, J. J.; Zakrzewski, V. G.; Dapprich, S.; Daniels, A. D.; Strain, M. C.; Farkas, O.; Malick, D. K.; Rabuck, A. D.; Raghavachari, K.; Foresman, J. B.; Ortiz, J. V.; Cui, Q.; Baboul, A. G.; Clifford, S.; Cioslowski, J.; Stefanov, B. B.; Liu, G.; Liashenko, A.; Piskorz, P.; Komaromi, I.; Martin, R. L.; Fox, D. J.; Keith, T.; Al-Laham, M. A.; Peng, C. Y.; Nanayakkara, A.; Challacombe, M.; Gill, P. M. W.; Johnson, B.; Chen, W.; Wong, M. W.; Gonzalez, C.; Pople, J. A. *Gaussian 03*, revision B.04; Gaussian, Inc.: Pittsburgh, PA, 2003.

(16) Dove, M. F. A.; Creighton, J. A.; Woodward, L. A. *Spectrochim. Acta* **1962**, *18*, 267.

(17) Abouaf-Marguin, L.; Jacox, M. E.; Milligan, D. E. *J. Mol. Spectrosc.* **1977**, *67*, 34.

(18) Nelander, B. *Chem. Phys.* **1984**, *87*, 283.

(19) Goldfarb, T. D.; Khare, B. N. *J. Chem. Phys*. **1967**, *46*, 3379.

(20) Purnell, C. J.; Barnes, A. J.; Suzuki, S.; Ball, D. F.; Orville-Thomas, W. J. *Chem. Phys*. **1976**, *12*, 77.

(21) Filgueira, R. R.; Fournier, L. L.; Varetti, E. L. *Spectrochim. Acta* **1982**, *38A*, 965.

(22) Ault, B. S. *J. Mol. Struct.* **2000**, *526*, 97.

(23) Ault, B. S. *Rev. Chem. Intermed.* **1988**, *9*, 233.

(24) Nakamoto, K., *Infrared and Raman Spectra of Inorganic and Coordination Compounds*; 5th ed.; Wiley-Interscience: New York, 1997.

(25) Barnes, A. J.; Hallam, H. E.; Scrimshaw, G. F. *Trans. Faraday Soc*. **1969**, *65*, 3150.

(26) Maillard, D.; Schriver, A.; Perchard, J. P. *J. Chem. Phys*. **1979**, *71*, 505.

(27) Ault, B. S. *Inorg. Chem*. **1981**, *20*, 2817.

(28) Ault, B. S., unpublished results.

(29) Henderson, W. G.; Taagepera, M.; Holtz, D.; McIver, R. T., Jr.; Beauchamp, J. L.; Taft, R. W. *J. Am. Chem. Soc*. **1972**, *94*, 4728.